

# Improved Supercontinuum Generation Through UV Processing of Highly Nonlinear Fibers

Paul S. Westbrook, Jeffrey W. Nicholson, Kenneth S. Feder, and Andrew D. Yablon, *Member, IEEE*

**Abstract**—We demonstrate that UV exposure of highly nonlinear, germano-silicate fibers can significantly broaden the infrared supercontinuum generated by femtosecond pulses in these fibers. Both simulations and measurements of the fiber chromatic dispersion show that UV-induced refractive index changes increase the waveguide dispersion by up to 5 ps/(nm-km) at 1570 nm and shift the dispersion zero by over 100 nm. We examine fibers with a range of UV exposure levels and show that the short wavelength edge of the supercontinuum can be continuously changed by more than 100 nm. We also show that the long wavelength edge is extended beyond that of the unexposed fiber. The resulting continuum spans from 0.85 to 2.6  $\mu\text{m}$ . Cutback measurements show that the supercontinuum in the exposed fiber is generated in as little as 1 cm of fiber. A nonlinear Schrödinger equation (NLSE) model of the supercontinuum generation in the nonlinear fiber shows that the short wavelength behavior of the continuum is primarily controlled by changes in the fiber dispersion caused by the UV-induced change in refractive index of the fiber core.

**Index Terms**—Fiber properties, nonlinear fibers, nonlinear optics, optical fabrication, pulse propagation and solitons.

## I. INTRODUCTION

**S**UPERCONTINUUM generation in bulk materials, as well as optical fibers, has been studied extensively [1]. In recent years, the development of novel optical waveguides with low and flat chromatic dispersion and very small effective area, as well as continuing improvements in pulsed laser sources has led to the observation of octave spanning (i.e., containing both  $f$  and  $2f$  frequencies) supercontinuum generation in the visible, as well as the infrared. Supercontinua extending to visible wavelengths are typically generated in micron-scale air-silica waveguides pumped by fs Ti-Sapphire lasers near 800 nm [2], [3], whereas infrared supercontinua [4] are frequently produced using erbium-doped femtosecond fiber lasers and germano-silicate highly nonlinear, dispersion-shifted fiber (HNLF) [5], [6]. The octave-spanning spectra generated in these systems have had significant impact on the field of frequency metrology. The supercontinuum is actually a comb of frequencies separated by the repetition rate of the pulsed laser driving the supercontinuum. An octave-spanning comb can then be readily referenced against itself by doubling the low frequency portion and beating against the high frequency portion, as has been demonstrated with bulk-optic solid-state lasers, [7] as well as more recently with fiber lasers [8]. The result is an ultrahigh

precision frequency ruler that has enabled vast improvements in absolute frequency measurements [9]. In addition to their useful frequency metrology properties, these sources exhibit very large spectral densities ( $> 0.1 \text{ mW/nm}$ ) over more than an octave of optical spectrum, making them useful in other technologies, such as optical coherence tomography [10], spectral slicing for telecommunication applications [11], swept wavelength Raman pumps [12], broadband spectral interferometry [13], and various other optical test and measurement applications that require intense ultrabroad-bandwidth sources. Despite their successes, though, fiber supercontinua have limitations, such as spectral flatness, noise, and bandwidth, that are dictated in part by the ability to design and fabricate a given fiber dispersion and nonlinearity. In particular, frequency metrology applications could benefit greatly by broadening the continuum to allow access to a wider range of stabilized atomic resonance frequencies. In addition, the necessity of less nonlinear fiber to span an octave for a given pump power could reduce the noise in the resulting continuum [14]. Moreover, nonuniform fiber dispersion profiles have been shown to give lower RIN noise [15], as well as broader bandwidth [16]. Such optimization is often achieved through lengthy fiber redesign/fabrication or cumbersome splicing of discrete fiber sections. More flexible methods of optimizing a fiber supercontinuum would allow for a broader range of supercontinuum sources to be designed and fabricated.

It is known that supercontinuum generation in optical waveguides depends on an interplay between the  $\chi_3$  optical nonlinearity and the dispersion of the waveguide. Control of the waveguide dispersion is usually achieved through careful design and fabrication of an appropriate fiber waveguide [6], [17], typically with very low dispersion and carefully chosen dispersion zero, in order to maintain narrow pulse shape and provide appropriate phase matching for nonlinear processes. While they often require meters of fiber, supercontinua have also been generated in centimeters of fiber [2], [3], [18]. Because the continuum generating fiber can be short, its light guiding properties can be significantly altered through various postprocessing techniques, thus greatly increasing the parameter space available for designing nonlinear fiber light sources.

One well-known postprocessing technique used to alter the nonlinear properties of an optical fiber is tapering of the outer diameter of the fiber. Similar to fiber draw, fiber tapering is achieved by applying tension to a heated fiber. It has been employed primarily to fabricate micron scale waveguides for use in visible supercontinuum generation [3]. While tapering is quite effective for this application, it is less desirable for tuning germanosilicate highly nonlinear fibers, since it has drawbacks

Manuscript received July 7, 2004; revised October 20, 2004.

The authors are with the OFS Labs, Somerset, NJ 08873 USA (e-mail: westbrook@ofsoptics.com).

Digital Object Identifier 10.1109/JLT.2004.840361

of mechanical fragility, intrusive high temperature/strain processing, nonstandard fiber diameters, and limited control in achieving nonuniform fiber diameters.

Another well-known fiber postprocessing technique employs UV radiation to increase the refractive index of the doped core of a fiber [19], [20]. UV photosensitivity is observed in many dopants and over a large range of UV wavelengths. For the Ge-doping in most silica fibers, UV near 248 nm is typically employed. By treating fibers with high pressure molecular hydrogen prior to exposure, UV irradiation can increase the core refractive index step ( $\Delta n$ ) by more than 10% [21]. UV exposure can be considered complementary to fiber tapering, since changes in the core refractive index are in general not equivalent to changes in the core diameter in fibers with complex radial refractive index profiles. Moreover, UV modification of the core refractive index is nonintrusive, since it can in some cases be accomplished without even removing the fiber coating [22]. It also allows a wide range of precisely controlled exposure profiles since a UV beam can easily have a diameter on the order of microns. Dispersion maps can then be written into a fiber using scanned exposure.

Control of fiber dispersion through UV postprocessing has several applications. As discussed above, experiments and simulations have shown that modifying the dispersion along the length of the continuum fiber can have a variety of benefits in the supercontinuum process, from broadening and flattening the continuum to reducing the relative intensity noise. In previous experiments, varying the dispersion was accomplished by splicing together sections of different HNLF with different dispersion properties [15]. UV control of fiber dispersion could allow substantial flexibility in designing a nonuniform dispersion along the fiber and eliminating splice losses in dispersion mapped HNLFs.

There are also practical limitations on the core  $\Delta n$  that can be achieved in the fiber manufacturing process and simply designing a new HNLF to have the same  $\Delta n$  as was obtained with UV exposure could be difficult. The small effective area and high nonlinearity of HNLF is achieved in part through high core-cladding index differences resulting from high core doping levels. However, large differences in the thermal expansion coefficients of a  $\text{GeO}_2$ -doped silica core and the silica cladding can cause the fiber preform to crack when the doping levels are very high. Various high  $\Delta n$  HNLF designs can approach this limit. Therefore, the increase in  $\Delta n$  obtainable with UV radiation ( $\sim 10\%$  in this paper) makes available a part of design space that was previously unavailable.

Finally, UV control of dispersion can achieve a range of dispersion values from a finite stock of fibers. As we show in this paper, the ability to dispersion tune a particular HNLF allows optimization of that fiber for a desired supercontinuum without the need for fiber redesign and refabrication. Moreover, analysis of an HNLF that has been optimized using UV exposure may be used in the redesign of a new optimized HNLF, thus decreasing the number of fiber preform iterations required to achieve a given design.

In this paper, we show that UV exposure of HNLF can significantly change its chromatic dispersion and thereby alter its

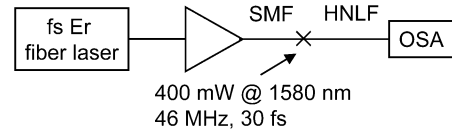


Fig. 1. Experimental setup of the supercontinuum source. SMF and HNLF are spliced at  $X$ .

supercontinuum generating properties. We use this fact to increase the supercontinuum bandwidth for a particular HNLF. We first record the dependence of supercontinuum generation in the HNLF as the UV dosage is varied, and show that the short wavelength edge of the continuum moves monotonically to shorter wavelengths as the fiber is exposed to increasing levels of UV. From our exposure study, we take one exposure level with enhanced supercontinuum bandwidth and examine both the long wavelength edge and perform a cutback measurement of the supercontinuum formation. The long wavelength edge of the continuum was observed to increase to  $2.6 \mu\text{m}$  making this supercontinuum span a range of frequencies that includes the third harmonic ( $0.85 \mu\text{m}$ ) of its longest wavelengths ( $2.55 \mu\text{m}$ ). The cutback measurement shows that the continuum can be generated in as little as 1 cm of UV exposed fiber and that the growth of the short-wavelength edge of the continuum saturates after approximately 3 cm of fiber. We also model our results with a nonlinear Schrödinger equation (NLSE) that includes  $\chi_3$  optical shock and delayed Raman terms in addition to self phase modulation [16], [23]. The chromatic dispersion is computed from simulations of the effective mode index using the measured fiber refractive index profile. To verify this chromatic dispersion we also measured the fiber dispersion using spectral interferometry and find good agreement with our simulated fiber dispersion. While the short wavelength edge of the continuum is well described using the measured chromatic dispersion, we find that long wavelength edge is not predicted accurately. We discuss that this may be due to inaccuracy of the fiber dispersion and nonlinearity at long wavelengths.

## II. SUPERCONTINUUM MEASUREMENTS

The setup of the supercontinuum source is shown in Fig. 1. The pump source was an amplified, modelocked Er-doped fiber laser, described in detail elsewhere [24]. The output of the amplifier was spliced to a length of HNLF (OFS Denmark); the output of the HNLF was directed into an optical spectrum analyzer (OSA). The fiber laser had a repetition rate of 46 MHz, pulse duration of 34 fs and average power of 0.4 W at the end of the single-mode fiber pigtail after the amplifier. Before exposure, the HNLF had a dispersion zero at 1478 nm, a dispersion at 1550 nm of  $1.19 \text{ ps}/(\text{nm}\cdot\text{km})$  and dispersion slope of  $0.009 \text{ ps}/(\text{nm}^2\cdot\text{km})$ , effective area of approximately  $13 \mu\text{m}^2$ , and a nonlinear coefficient of approximately  $10.6 \text{ W}^{-1}\text{km}^{-1}$ .

To study the effect of UV exposure, we exposed several lengths of HNLF to increasing levels of UV radiation. The fiber was first photosensitized with high pressure  $D_2$ . The coating was then removed and the UV exposure was achieved by scanning a focused beam from an excimer laser at 248 nm across the stripped fiber. The pulse duration was  $\sim 20 \text{ ns}$ , the repetition rate was 30 Hz, and the intensity at the fiber was

$\sim 200 \text{ mJ/cm}^2$  pulse. Several dosages were used. In all figures a “full exposure” corresponds to roughly  $2 \text{ kJ/cm}^2$ . Other exposure levels are referenced to this value. The exposure length for each fiber was 8 cm. The refractive index of the fiber core was measured to increase by  $\sim 0.004$  after the full UV exposure, whereas the index of the cladding was left unchanged. To obtain a measure of the change in refractive index with UV exposure, we wrote a Bragg grating in the fiber and observed the change in its resonant wavelength as the fiber was exposed. The Bragg resonance wavelength is proportional to the effective mode index, which is less than and roughly proportional to the core refractive index. The change in core mode effective index is shown in Fig. 2(c). The  $x$ -axis units are normalized to the full exposure level. The Bragg wavelength was 1570 nm.

Fig. 2(a) shows the continuum measured in 5 fibers with exposure levels of 0, 1/4, 1/2, 1, and 2 times the full exposure level. The short wavelength edge is observed to shift uniformly to shorter wavelengths as the exposure level is increased. Fig. 2(b) shows the trend for the short wavelength edge of the continuum. Increasing the UV dose causes a continuous increase in the short wavelength edge of the continuum, until the effect saturates at roughly twice the full exposure level. The short wavelength edge had a small dependence on the polarization of the light launched into the HNLF. The maximum and minimum measured short wavelength edge for each exposure level is plotted in Fig. 2(b) as an error bar. Note that these do not correspond to an unstable or ill-defined short wavelength edge. A polarized launch into the fiber gave a stable short wavelength edge. The saturation of the short wavelength edge may be partly attributed to decreased index change after the full exposure level, as seen in Fig. 2(c). However, the effective index continued to change even with three times the full exposure level. Therefore, the saturation may also be due to decreased sensitivity of the fiber dispersion after full exposure. A redesign of this fiber for optimal supercontinuum bandwidth could employ this observed saturation as a guideline for setting an optimal Ge-doping level.

We then examined the fully exposed fiber further and compared its performance to the unexposed fiber. Fig. 3 shows the long wavelength edge of the fully exposed fiber compared to the unexposed fiber. Note that the long wavelength edge of the continuum is also extended substantially. The continuum in the exposed fiber is broad enough to encompass both a fundamental frequency,  $f$  ( $2.55 \mu\text{m}$ ) and its third harmonic,  $3f$  ( $0.85 \mu\text{m}$ ). The existence of both  $f$  and  $3f$  in the same frequency comb would in principle allow carrier envelope stabilization using the  $\chi_3$  optical nonlinearity in the silica fiber, since the third harmonic generation has previously been observed in nonlinear fibers [25], [26]. We note, however, that the core-cladding index contrast in our HNLF may be too small for phase matching of the third harmonic into a guided mode [26]. Therefore, other phase matching means may be necessary to excite the third harmonic. Moreover, appropriate dispersive means (e.g., an interferometer and/or grating) would also be necessary to ensure that the continuum and the third harmonic had sufficient temporal overlap to produce the beat note necessary for carrier envelope stabilization.

Fig. 4 shows a cutback measurement of the supercontinuum generation in the unexposed and fully exposed fibers. Clearly

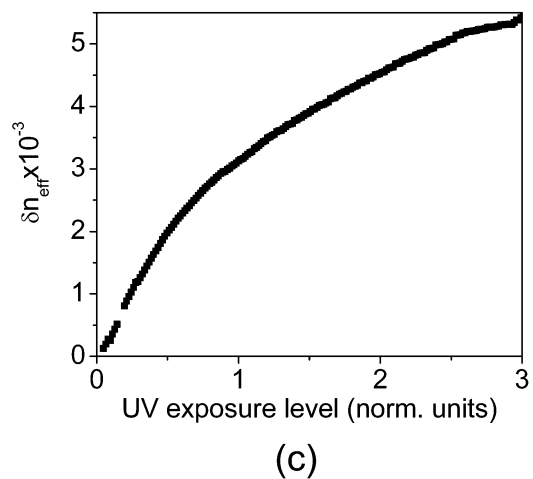
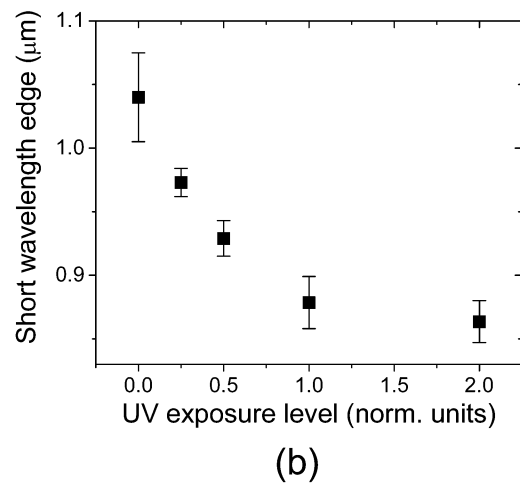
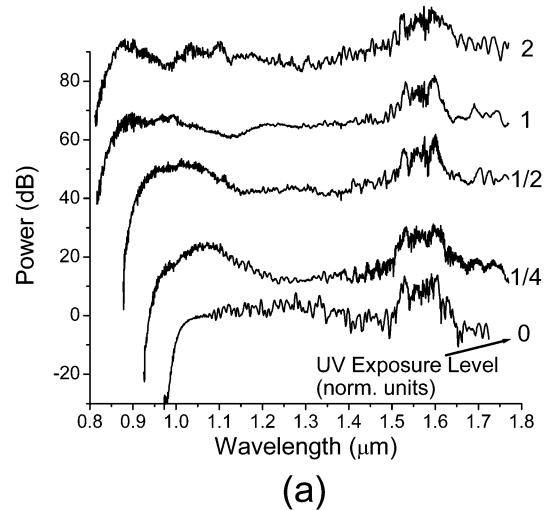


Fig. 2. (a) Continuum generation HNLf with varying UV exposure level, labeled next to each plot in units normalized to full exposure:  $\sim 2 \text{ kJ/cm}^2$ . Curves have been offset vertically for clarity. (b) Shift in the short wavelength edge of the continuum as a function of exposure level. Bars indicate the range of the short wavelength edge with launch polarization. Short wavelength edge was stable with a fixed input launch polarization. (c) Change in effective index of core mode at 1570 nm with UV exposure. Measured using Bragg grating in HNLF.

the supercontinuum is generated quite rapidly in the exposed fiber when compared to the unexposed fiber. Moreover, the supercontinuum short wavelength edge in both fibers remains the

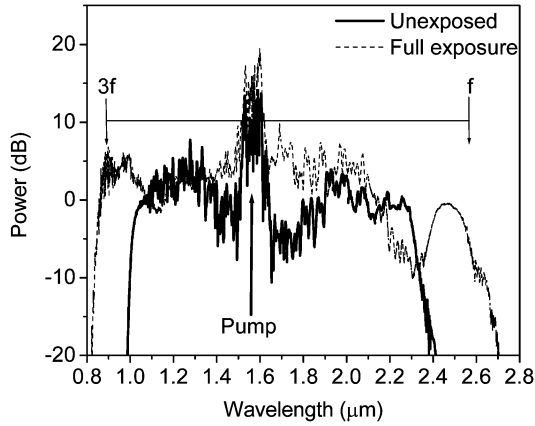


Fig. 3. Long wavelength edge of supercontinuum measured in fully exposed and unexposed fibers. Note that the exposed fiber contains both a fundamental frequency  $f$  ( $2.55 \mu\text{m}$ ) and its third harmonic  $3f$  ( $0.85 \mu\text{m}$ ).

same after about 3 cm of fiber. This saturation of the short wavelength edge was found to occur in many fibers, as well as in simulations of the supercontinuum generation. Generation of bandwidth in such short lengths of fiber may have implications in reducing noise in frequency metrology applications [14].

### III. FIBER CHROMATIC DISPERSION MEASUREMENTS

While we have focused on changes in the chromatic dispersion of the fiber, there could be a number of effects leading to the observed enhancement in the continuum. It may be due to a change in waveguide dispersion, mode field diameter, or the linear and nonlinear susceptibility of the UV exposed germanosilicate fiber core, or to some combination of these effects. To better understand which of these is of greatest significance, we performed simulations of the continuum generation using only the chromatic dispersion and effective area changes. We first calculated the dispersion and effective area of the UV exposed HNLF from the measured fiber refractive index profile. The calculated dispersion of the fiber, before and after UV exposure, is plotted in Fig. 5. To verify that the dispersion simulated from the measured profile was correct, we also measured the fiber dispersion using spectral interferometry [27]. The fiber was placed in one arm of a Mach-Zehnder interferometer and a supercontinuum source was launched into the interferometer. An OSA was used to observe the fringes at the output, and analysis of these fringes yielded the fiber dispersion. The dispersion of the interferometer optics was ignored, but rough fiber cutback measurements showed a small systematic error of  $\sim 0.6 \text{ fs/nm}$  maximum and  $\sim 0.3 \text{ fs/nm}$  average dispersion due to the interferometer optics. Both unexposed and fully exposed fibers were measured. The lengths were 237 and 213 mm, respectively. The symbols in Fig. 5 show these measurements and they agree with the calculated dispersion that was used in the NLSE simulations. In particular, the dispersion zeros of the two fibers were roughly 125 nm apart and matched the simulated values fairly well. Note that the simulations required dispersion over a large range (0.4 to  $3 \mu\text{m}$ ), so the experimentally measured values could not be used. Fig. 5(b) shows the simulated fiber dispersion over a much larger wavelength range. The simulations also yielded effective area values necessary for the NLSE simulations. The effective

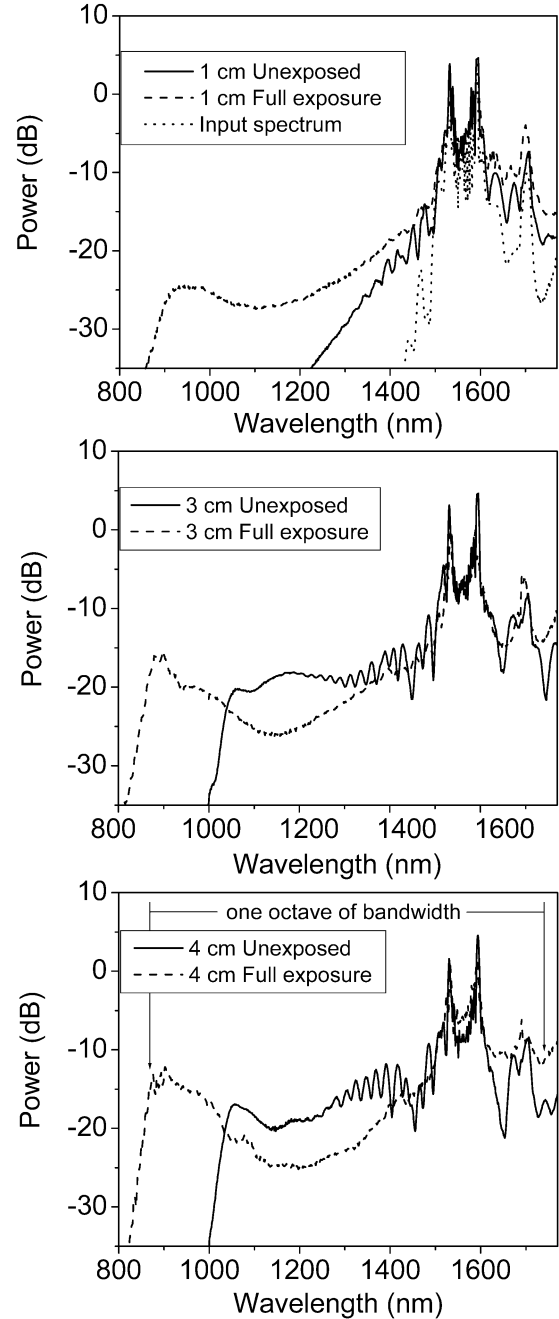


Fig. 4. Cutback measurements showing the evolution of the supercontinuum in both the fully exposed and the unexposed fibers. Continuum is generated much more rapidly in the exposed fiber and both continua stabilize after roughly 3 cm.

areas were  $13.48 \mu\text{m}^2$  before and  $12.89 \mu\text{m}^2$  after full UV exposure.

### IV. NLSE SIMULATIONS

These waveguide parameters were then used in a NLSE simulation of the nonlinear propagation in the fiber waveguide. This simulation, based on the standard split step Fourier method, has been used previously to successfully simulate continuum generation in dispersion mapped, HNLFs [16]. As aforementioned, in this simulation, changes to both dispersion and effective area caused by UV exposure were included, but the nonlinear susceptibility was assumed unchanged. The resulting su-

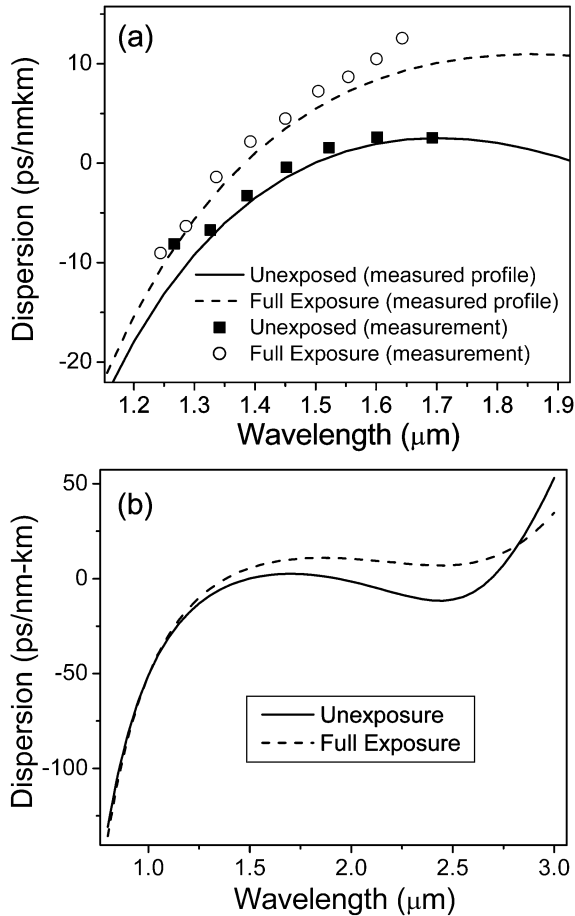


Fig. 5. (a) Chromatic dispersion in the unexposed and fully exposed fibers. Lines are simulations using the measured fiber refractive index profile. Symbols are measured values using spectral interferometry. Fiber lengths: 237 mm, unexposed and 213 mm fully exposed. (b) Simulated chromatic dispersion values over a larger wavelength range.

percontinua after 12 cm of UV exposed fiber (solid line) compared to 12 cm of unexposed HNLf (dashed line) are shown in Fig. 6. These plots show that most of the increase in the supercontinuum bandwidth on the short wavelength side can be accounted for by taking only the waveguide parameters into account. Therefore, we expect that the enhanced short wavelength edge of the continuum was likely not the result of a large change in germanosilicate nonlinear susceptibility after UV irradiation. Simulations in which the  $\chi_3$  of the fiber were also changed only caused minor increases on the short wavelength side of the continuum, changes that were less than the experimentally observed polarization dependence in Fig. 2. Therefore, while these simulations show that the primary cause for the enhancement in the short wavelength edge of the continuum is due to dispersion changes, they do not rule out the possibility that the HNLf also shows a change in  $\chi_3$  after UV exposure.

The long wavelength edge of the exposed fiber did not increase in our simulation. This is not in agreement with the data of Fig. 3 which shows an increase of the long wavelength edge. We attribute this disagreement to our uncertainty about the chromatic dispersion, effective area and  $\chi_3$  at wavelengths beyond 2 μm. In the simulations,  $\chi_3$  and the effective area were assumed to be constant. Improved simulations of the long wavelength

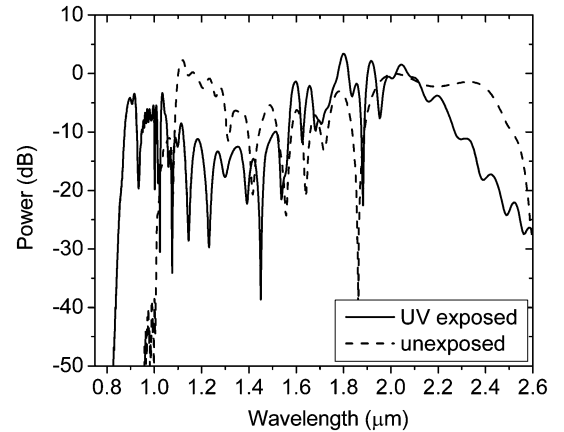


Fig. 6. NLSE simulations of supercontinuum generation in 12 cm fully UV exposed and unexposed HNLf. Chromatic dispersions are shown in Fig. 5. Effective areas were  $13.48 \mu\text{m}^2$  unexposed and  $12.89 \mu\text{m}^2$  full UV exposure. Nonlinear susceptibility is the same in each case.

edge are likely to yield more information about the changes in  $\chi_3$  after UV irradiation.

## V. CONCLUSION

In conclusion, we have demonstrated the effectiveness of UV exposure for altering and enhancing continuum generation in optical fibers. We applied this technique to improve a particular HNLf for maximum supercontinuum bandwidth. This HNLf showed a greater than 100 nm shift in both the dispersion zero and short wavelength continuum edge, and more than 5 ps/nmkm of change in chromatic dispersion at 1570 nm. The exposed fiber produced a continuum spanning from 0.85 μm to 2.6 μm, a range that includes the third harmonic of its lowest frequencies. By varying the fiber exposure level we were able to obtain a range of supercontinuum bandwidths, thus using a single fiber to achieve a set of supercontinua that would normally require several distinct fibers. To ascertain the origins of the supercontinuum enhancement, we measured the fiber chromatic dispersion using spectral interferometry as well as simulations from the measured fiber refractive index profile. These results agreed and the simulated results were used in a NLSE model of the supercontinuum generation. The enhancements on the short wavelength edge were largely accounted for by including only the altered chromatic dispersion in this NLSE model. However, changes to the long wavelength edge were not well described, and require inclusion of more accurate wavelength dependence of the parameters in the NLSE simulations.

## ACKNOWLEDGMENT

The authors would like to thank M. F. Yan and J. Jasapara for helpful discussion.

## REFERENCES

- [1] R. R. Alfano, Ed., *The Supercontinuum Laser Source*. New York: Springer-Verlag, 1989.
- [2] J. K. Ranka, R. S. Windeler, and A. J. Stentz, "Visible continuum generation in air-silica microstructure optical fibers with anomalous dispersion at 800 nm," *Opt. Lett.*, vol. 25, no. 1, pp. 25–27, Jan. 2000.

- [3] T. A. Birks, W. J. Wadsworth, and P. St. J. Russell, "Supercontinuum generation in tapered fibers," *Opt. Lett.*, vol. 25, no. 19, pp. 1415–1417, Oct. 2000.
- [4] J. W. Nicholson, M. F. Yan, P. Wisk, J. Fleming, F. DiMarcello, E. Monberg, A. Yablon, C. Jørgensen, and T. Veng, "All-fiber, octave-spanning supercontinuum," *Opt. Lett.*, vol. 28, no. 8, pp. 643–645, Apr. 2003.
- [5] T. Okuno, M. Onishi, T. Kashiwada, S. Ishikawa, and M. Nichimura, "Silica-based functional fibers with enhanced nonlinearity and their applications," *IEEE J. Sel. Topics Quantum Electron.*, vol. 5, pp. 1385–1391, Sep.–Oct. 1999.
- [6] C. G. Jørgensen, T. Veng, L. Gruner-Nielsen, and M. Yan, "Dispersion flattened highly nonlinear fiber," in *Proc. 29th Europ. Conf. Opt. Commun., ECOC '03*, Rimini, Italy, pp. 556–557.
- [7] D. J. Jones, S. A. Diddams, J. K. Ranka, A. Stentz, R. S. Windeler, J. L. Hall, and S. T. Cundiff, "Carrier-Envelope phase control of femtosecond mode-locked lasers and direct optical frequency synthesis," *Science*, vol. 288, pp. 635–639, Apr. 2000.
- [8] B. R. Washburn, S. A. Diddams, N. R. Newbury, J. W. Nicholson, M. F. Yan, and C. G. Jørgensen, "Phase-locked erbium-fiber-laser-based frequency comb in the near infrared," *Opt. Lett.*, vol. 29, no. 3, pp. 250–252, Feb. 2004.
- [9] L. S. Ma, Z. Y. Bi, A. Bartels, L. Robertsson, M. Zucco, R. S. Windeler, G. Wilpers, C. Oates, L. Hollberg, and S. A. Diddams, "Optical frequency synthesis and comparison with uncertainty at the  $10^{-19}$  level," *Science*, vol. 303, pp. 1843–1845, Mar. 2004.
- [10] I. Hartl, X. D. Li, C. Chudoba, R. K. Ghanta, T. H. Ko, J. G. Fujimoto, J. K. Ranka, and R. S. Windeler, "Ultrahigh-resolution optical coherence tomography using continuum generation in an air silica microstructure optical fiber," *Opt. Lett.*, vol. 26, no. 9, pp. 608–610, May 2001.
- [11] S. Kawanishi, H. Takara, K. Uchiyama, I. Shake, and K. Mori, "3 Tbit/s (160 Gbit/s  $\times$  19 channel) optical TDM and WDM transmission experiment," *Electron. Lett.*, vol. 35, no. 10, pp. 826–827, May 1999.
- [12] J. W. Nicholson, J. M. Fini, J.-C. Bouteiller, J. Bromage, and K. Brar, "Stretched ultrashort pulses for high repetition rate swept-wavelength Raman pumping," *J. Lightw. Technol.*, vol. 22, pp. 71–78, Jan. 2004.
- [13] J. Jasapara, T. H. Her, R. Bise, R. Windeler, and D. J. DiGiovanni, "Group-velocity dispersion measurements in a photonic bandgap fiber," *J. Opt. Soc. Am. B*, vol. 20, no. 8, pp. 1611–1615, Aug. 2003.
- [14] K. L. Corwin, N. R. Newbury, J. M. Dudley, S. Coen, S. A. Diddams, B. R. Washburn, K. Weber, and R. S. Windeler, "Fundamental amplitude noise limitations to supercontinuum spectra generated in microstructure fiber," *Appl. Phys. B*, vol. 77, pp. 269–269, 2003.
- [15] T. Hori, J. Takayanagi, N. Nishizawa, and T. Goto, "Flatly broadened, wideband and low noise supercontinuum generation in highly nonlinear hybrid fiber," *Opt. Expr.*, vol. 12, no. 2, pp. 317–324, Jan. 2004.
- [16] J. W. Nicholson, A. K. Abeeluck, C. Headley, M. F. Yan, and C. G. Jørgensen, "Pulsed and continuous-wave supercontinuum generation in highly nonlinear, dispersion-shifted fibers," *Applied Physics B*, vol. 77, pp. 211–218, 2003.
- [17] W. H. Reeves, D. V. Skryabin, F. Biancalana, J. C. Knight, P. St. J. Russell, F. G. Omenetto, A. Efimov, and A. J. Taylor, "Transformation and control of ultra-short pulses in dispersion-engineered photonic crystal fibers," *Nature*, vol. 424, pp. 511–515, Jul. 2003.
- [18] F. Tauser, A. Leitenstorfer, and W. Zinth, "Amplified femtosecond pulses from an Er:Fiber system: Nonlinear pulse shortening and self referencing detection of the carrier-envelope phase evolution," *Opt. Expr.*, vol. 11, no. 6, pp. 594–600, Mar. 2003.
- [19] K. O. Hill, Y. Fujii, D. C. Johnson, and B. S. Kawasaki, "Photosensitivity in optical waveguides: Application to reflection filter fabrication," *Appl. Phys. Lett.*, vol. 32, no. 10, pp. 647–649, May 1978.
- [20] J. W. Nicholson, P. S. Westbrook, K. S. Feder, and A. D. Yablon, "Supercontinuum generation in ultraviolet-irradiated fibers," *Opt. Lett.*, vol. 29, no. 20, pp. 2363–2365, Oct. 2004.
- [21] R. Kashyap, *Fiber Bragg Gratings*. New York: Academic Press, 1999.
- [22] D. A. Simoff, R. P. Espindola, M. A. Paczkowski, R. M. Atkins, N. P. Wang, and A. Hale, "UV-Transparent coatings for the fabrication of optical fiber gratings," *Polym. Preprints*, vol. 40, no. 2, pp. 1289–1290, Aug. 1999.
- [23] G. P. Agrawal, *Nonlinear Fiber Optics*, second ed. San Diego, CA: Academic, 1995, ch. 2.
- [24] J. W. Nicholson, A. D. Yablon, P. S. Westbrook, K. S. Feder, and M. F. Yan, "High power, single mode, all-fiber source of femtosecond pulses at 1550 nm and its use in supercontinuum generation," *Opt. Expr.*, vol. 12, no. 13, pp. 3025–3034, June 2004.
- [25] J. K. Ranka, R. S. Windeler, and A. J. Stentz, "Optical properties of high-delta air-silica microstructure optical fibers," *Opt. Lett.*, vol. 25, no. 11, pp. 796–798, Jun. 2000.
- [26] A. Efimov, A. J. Taylor, F. G. Omenetto, J. C. Knight, W. J. Wadsworth, and P. St. J. Russell, "Phase-matched third harmonic generation in microstructured fibers," *Opt. Expr.*, vol. 11, no. 20, pp. 2567–2576, 2003.
- [27] H. Shang, "Chromatic dispersion measurement by white-light interferometry on meter-length single-mode optical fibers," *Electron. Lett.*, vol. 17, no. 17, pp. 603–605, Aug. 1981.



**Paul S. Westbrook** received the B.S. degree in physics from the University of Michigan in 1990 and the Ph.D. degree from the Massachusetts Institute of Technology, Cambridge, also in physics, in 1998.

He then joined Lucent Technologies Bell Laboratories as a Postdoctoral researcher, and later, Member of Technical Staff in the Optical Fiber Research Department. He has been Technical Manager of OFS Labs' Gratings and Devices group since 2001 when Bell Labs optical fiber research was sold to Furukawa and became OFS Labs. He has worked on several

topics in optical physics, including photoresponse of superconductors, optical fiber gratings, polarization measurement, and microstructured optical fibers.



**Jeffrey W. Nicholson** was born in Louisville, KY, in 1969. He received the B.S. degree in physics from the University of Houston, Houston, TX, in 1991 and the Ph.D. degree in optical sciences from the University of New Mexico, Albuquerque, in 1997.

After graduation, he worked as a Postdoctoral researcher with Los Alamos National Laboratory in the area of short pulse propagation and with Directed Energy Solutions, Albuquerque, in the area of high power gas lasers. Since 2000, he has been with Bell Labs, and then OFS Labs as a Member of Technical

Staff in the Optical Fiber Research Group, in Murray Hill, NJ. His current interests include fiber lasers and amplifiers and nonlinear propagation effects in fibers.

**Kenneth S. Feder**, photograph and biography not available at the time of publication.



**Andrew D. Yablon** (M'03) was born in New York City on December 22, 1970. He received the S.B. degree in 1992, the S.M. degree in 1993, and the Ph.D. degree in 1997, all in mechanical engineering, from the Massachusetts Institute of Technology, Cambridge.

From 1998 to 2000, he was a Senior Research Scientist with Vytran Corporation, Morganville, NJ, where he developed novel fiber processing and fusion splicing technologies. Since 2000 he has been a Member of Technical Staff at OFS Laboratories,

Murray Hill, NJ (formerly the Optical Fiber Research Department of Bell Laboratories, Lucent Technologies). His current research interests include optical fiber coupling technologies, fusion splicing, and fiber refractive index measurements.

Dr. Yablon is a member of the OSA and ASME.